Version of Record: https://www.sciencedirect.com/science/article/pii/S0032591022005952
Manuscript_163b38239e4dcb74708155bf5e734814

Packing density of limestone calcined clay binder

Baptiste Luzu[1*], Romain Trauchessec[1] and André Lecomte[1]

[*]baptiste.luzu@univ-lorraine.fr

[1] Université de Lorraine, CNRS, Institut Jean Lamour UMR 7198, F-54000 Nancy

The partial substitution of Portland cement by a mixture of calcined clays and limestone fillers offers a promising way to reduce the environmental impact of concrete while improving its long-term mechanical performance and durability properties. However, the literature shows that calcined clays can display a higher water demand than Portland cement, which implies the use of additional mixing water or superplasticizer to maintain appropriate workability. This study aims to determine the optimal proportion of ternary mixes, i.e. cement, calcined clays and limestone fillers, in order to obtain the highest possible packing density influencing the water demand. The associated experiments were conducted with one CEM I, two metakaolins (calcined clay) and three limestone fillers. Optimization was performed using the Compressible Packing Model of granular mixtures, which notably considers the grain size distribution and virtual packing densities (β_i) of the various materials. In conjunction with this model, the tests carried out on pastes of normal consistency controlled by the Vicat apparatus or the spread of mortars show that the type and amount of metakaolin used have a high impact on compactness given their particularly low virtual packing densities (β_i). Moreover, this study demonstrates that the addition of limestone fillers improves packing density, but the grain size distribution proves not to be the key parameter, especially in mortars. Lastly, when the water demand of the metakaolin is high, a large limestone proportion (30% vol.) allows significantly enhancing the spread and manufacturing mortars with a compressive strength of close to 32.5 MPa at 28 days.

Keywords: Limestone, calcined clay, packing density, Compressible Packing Model, normal consistency.

1. Introduction

In the aim of reducing the environmental impact of cementitious materials, research over the past several years has focused on the substitution of Portland clinker by calcined clay and limestone [1–10]. This kind of new material, called LC3-50 for limestone Calcined Clay Cement, allows for the replacement of up to 50 wt% of the clinker by 30 wt% of calcined clay, 15 wt% of limestone and 5 wt% of gypsum [11], [12]. In comparison with pure Portland cement (CEM I), given the lower calcination temperature of clays (≈ 850°C) and the absence of decarbonation, the CO_2 emissions per ton of LC3-50 binder can be reduced by approx. 30% [13]. Along these lines, Standard EN 197-5 [14] authorizes the use of such a high amount of limestone (LL) and natural calcined pozzolan (Q) additions (up to 50 wt%) for Portland-composite cement, called CEM II/C-M (Q-LL). In concrete, depending on the exposure class, the limestone or metakaolin (i.e. calcined kaolinite) can also be added with CEM I or CEM II/A to form the binder, which takes into account the activity (k-factor) of the addition [15].

Moreover, most calcined clays display good reactivity, and the clay deposits are widely available. The limestone is available in huge quantities at a low price, and the grinding process during its production consumes little energy. This process improves workability in the fresh state as well as the early strength of the hardened material by providing surface nucleation for hydrates; this step involves the formation of additional hydrates by reaction with aluminates [13,16,17].

However, the calcined clays used in this particular mix design have a water demand greater than that of cement and limestone filler. In addition, the amount of superplasticizer required to yield a good workability is high, reaching 3% [18]. This superplasticizer addition is not in accordance with an approach that promotes a smaller environmental impact and moreover increases the cost.

This effect of calcined clay is owed to the specificities (fineness, surface charges, etc.) of this kind of addition, which affects blend packing density. A better characterization of calcined clay properties and their impact on packing density can serve to optimize the various addition proportions and fineness, thereby favoring the use of this binder. Consequently, this study proposes to evaluate the impact of the

amount and physical properties of the Supplementary Cementitious Materials (SCMs, i.e. metakaolin (MK) and limestone (L)) on water demand (w/p: water/powder weight ratio), which directly controls the packing density Φ of the granular skeleton of the mix via the following relation (Equation 1) [19]:

$$\Phi = \frac{1}{1 + \rho_p \frac{w}{p}} \quad (1)$$

where ρ_p is the specific gravity of the powder.

The experimental packing density Φ has always been measured with the method proposed in [20], as inspired from Standard NF EN 196-3 [21], which implies use of the Vicat apparatus and a consistency probe in order to determine the quantity of water (and thus the packing density) needed to reach normal consistency. The consistency of a cementitious paste is considered to be normal if, at 4 minutes after a given mixing protocol and filling of a conical mold, the consistency probe inserted vertically into the fresh paste reaches 6 mm ± 2 mm from the bottom of the mold. A slight variation in the amount of water implies a great difference with respect to the penetration length where the probe stops. This method avoids any subjective determination of consistency [20,22].

In order to numerically predict the evolution of the packing density of both binary and ternary blends relative to the amount and properties of the constituents (cementitious materials), the Compressible Packing Model (CPM) developed in [19] appears to be relevant, according to [20] and [22]. This model enables determining the packing density of a granular skeleton blend composed with poly-sized material, including the fine and even ultrafine fractions. It relates the packing index K (which describes the degree of mixture compaction) with the packing density Φ by the following equation (Equation 2):

$$K = \sum_{i=1}^{n} \frac{\frac{y_i}{\beta_i}}{\frac{1}{\Phi} - \frac{1}{\gamma_i}} \quad (2)$$

where y_i and β_i are respectively the volume fraction and virtual packing density of the *n* elementary granular classes in the blend, and γ_i is the virtual packing density of the mixture where *i* is considered as the dominant granular class.

The virtual packing density β_i of a monodisperse class *i* is defined as the maximum compactness that can be expected from the deterministically arranged stack of grains [19].

For example, for a stack of spheres, the corresponding arrangement is the compact hexagonal stack, and the corresponding virtual packing density equals 0.74. For rough, non-spherical natural grains, the virtual compactness generally reaches a lower value. This numerical parameter globally considers the properties that physically affect the ability of grains to stack efficiently, such as shape, roughness and surface charges; it is widely used in this study to compare and explain the behavior of the materials studied.

The packing index, K, is an increasing function resulting from the summation of the partial packing index K_i of each individual granular class, as shown in Equation 3 below:

$$K = \sum_{i=1}^{n} K_i = \sum_{i=1}^{n} \frac{\frac{\phi_i}{\phi_i^*}}{1 - \frac{\phi_i}{\phi_i^*}} \quad (3)$$

where Φ_i is the real volume of class *i* and Φ_i^* the maximum volume potentially occupied by granular class *i* in the presence of other grains.

Relation (2) shows that when packing density $\Phi = \sum_{i=1}^{n} \Phi_i$ increases and is close to the virtual packing density γ, the packing index K also increases and tends to infinity. Thus, a unique value of K exists and serves to characterize the degree of compaction for each value of Φ. The expression of γ_i and Φ_i^* can be found in [19].

This model is able to accurately estimate the real packing density of a mixture that includes a large number of aggregates spanning all types and all granular classes. As explained above, its reliability is due in particular to use of the virtual packing density β_i, which takes into account the morphology and texture of the particles of each elementary class. This virtual packing density, usually considered to be uniform over the granular skeleton of the fine material, is determined with the CPM thanks to the real packing density measurement Φ conducted on the constituents of a mixture under calibrated and

reproducible conditions, i.e. where packing index K is known. The packing index used for the mixing protocol in this study (paste with normal consistency) was determined by [20] as equal to 4.8.

Recently, many works have described a new method to determine the wet packing density of cement or cementitious materials either with our without superplasticizer [23–26]. This method implies a gradual addition of the solid part to maintain its saturation as long as possible during the mixing process in order to avoid particle agglomeration. The void ratio is then derived for each water/(powder) ratio, and the mixture with the lowest void ratio is considered to have the best packing density. Moreover, for this method, the packing index used as an input into the CPM was equal to infinity since it was considered that the particular mixing process enabled obtaining perfect particle compaction [23–26]. Moreover, several models have been developed to simulate the packing density of mono-sized spherical particle mixtures [27,28], poly-sized spherical particle mixtures [19] or angular aggregate particle mixtures [29]. Their accuracy has been compared with various experimental datasets of spherical micro-powder mixtures of different sizes [24,30,31].

Nevertheless, for purposes of this study, it has been considered more convenient and sufficiently accurate to use of the Compressible Packing Model (CPM) and the standard mixing process of cement paste, thus implying a constant packing index (K) of 4.8. The packing density of several additional cementitious materials could thereby be determined, namely for three limestone fillers and two metakaolins. Their combination with CEM I cement was optimized, in seeking to increase the packing density of the resulting limestone calcined clay binders, so as to limit their water demand without a superplasticizer or preserve mortar workability in the fresh state. Special emphasis is paid to the impact of limestone fineness in order to control workability. This article also confirms the relevance of the compressible packing model for predicting the packing density of cement pastes containing calcined clays and for optimizing mixes.

2. Materials and methods

2.1. Materials

The physical properties of the materials used for this study are displayed in Table 1. The cement used was a CEM I 52.5 N. Two metakaolins (MK) were tested. The first, called M1, is a very pure metakaolin (Argical M1000®) available on the market; it contains low amounts of quartz and muscovite, as shown in Figure 1 by X-ray diffraction performed with a Bruker D8 Advance ($k_{\alpha(Cu)}$ = 1.54506 Å). The data were collected in 2θ intervals from 5° to 80°, with a step of 0.029°. The different mineral phases were identified using the EVA® software. This metakaolin was calcined in a rotary kiln and then crushed until achieving a very fine particle size distribution, with d50 = 6.6 µm (Figure 2). The particle size distribution (PSD) of the fine fraction (< 100 µm) was measured with an HELOS (H2802) laser diffraction particle sizer equipped with a RODOS® dispersion system, produced by Sympactec GmbH. The curve obtained is the average of three measurements recorded using two lenses. For the fraction above 100 µm, the PSD was measured with sieves of 2 mm - 1 mm - 500 µm - 250 µm - 200 µm - 160 µm - 125 µm and 100 µm. As seen in Table 1, its Blaine specific surface area, as measured according to Standard NF EN 196-6 [32], reaches 2.30 m²/g. This high value could be confirmed by the BET_{SSA} measurement, i.e. 19.40 m²/g, as determined from adsorption isotherms (N_2 77K) collected using a Micromeritics ASASP 2020 adsorption apparatus. The samples were first degassed at 400°C for 12 h, and the BET (Brunauer-Emmet-Taylor) apparent surface area was determined over the range of the N_2 relative pressure (P/P_0), extending from 0.05 to 0.18. Figure 3a shows that metakaolin M1 is composed of numerous aggregated metakaolin particles of various sizes. This Scanning Electron Microscopy (SEM) observations were generated by a FEI ® Quanta 650 equipped with a Field Emission Gun (FEG). The samples were covered with carbon to both allow for better electron conduction and obtain a higher quality quantification of the chemical elements. The properties of the second metakaolin, named M2, are very different. This specimen was produced with a flash calcination step by Argicem (France) and contains a large quantity of quartz, as deduced from the X-ray diffraction pattern (Figure 1) or from Figure 3c, which shows the numerous quartz particles (in red) in M2. These particles are often recovered by clay sheets, as observed in Figures 3e and 3f.

The Blaine specific surface area of M2, i.e. equal to 0.57 m²/g, is significantly less than that of M1, 2.30 m²/g, and its d50 of around 20 µm (Table 1) also confirms the presence of coarser quartz particles.

Three limestone fillers with distinct origins and particle size distributions were used. The coarser one (L1) was prepared in the lab by crushing coarse limestone smaller than 2 mm with a jaw crusher and then grinding for 45 minutes at 65 rpm (revolutions per minute) with a planetary mill (Resch model with a ball/powder ratio equal to 4.0). Lastly, the powder was sieved at 250 µm in order to attain a Blaine specific surface area of around 0.35 m²/g. Its mineralogical analysis in Figure 1 reveals that L1 is highly pure with low amounts of dolomite (MgO) and quartz (SiO_2). The two other limestone fillers were industrially produced; they are composed of 99% calcite. The Betocarb HP ® (L2) has a d50 equal to 3.8 µm and a Blaine of 0.56 m²/g, while the Betocarb F®, denoted L3, is the finest limestone filler with a d50 equal to 1.8 µm and a Blaine specific surface area greater than 1.0 m²/g.

The sand used is the siliceous 0/2 sand described in Standard NF EN-196-1 [33].

Table 1: Physical properties of the different materials used in this study

Material	***Density (g/cm³)***	***Blaine SSA (m²/g)***	***d50 (µm)***	***BET (m²/g)***
CEM I	3.19	0.5	7.5	2,56
M1	2.62	2.3*	6.6	19,45
M2	2.63	0.56*	19.9	15,95
L1	2.75	0.29	60.9	1,66
L2	2.7	0.56	3.8	1,17
L3	2.7	1.04	1.8	2,43

** porosity = 0.65 for M1 and 0.6 for M2 (porosity = 0.5 for all others materials)*

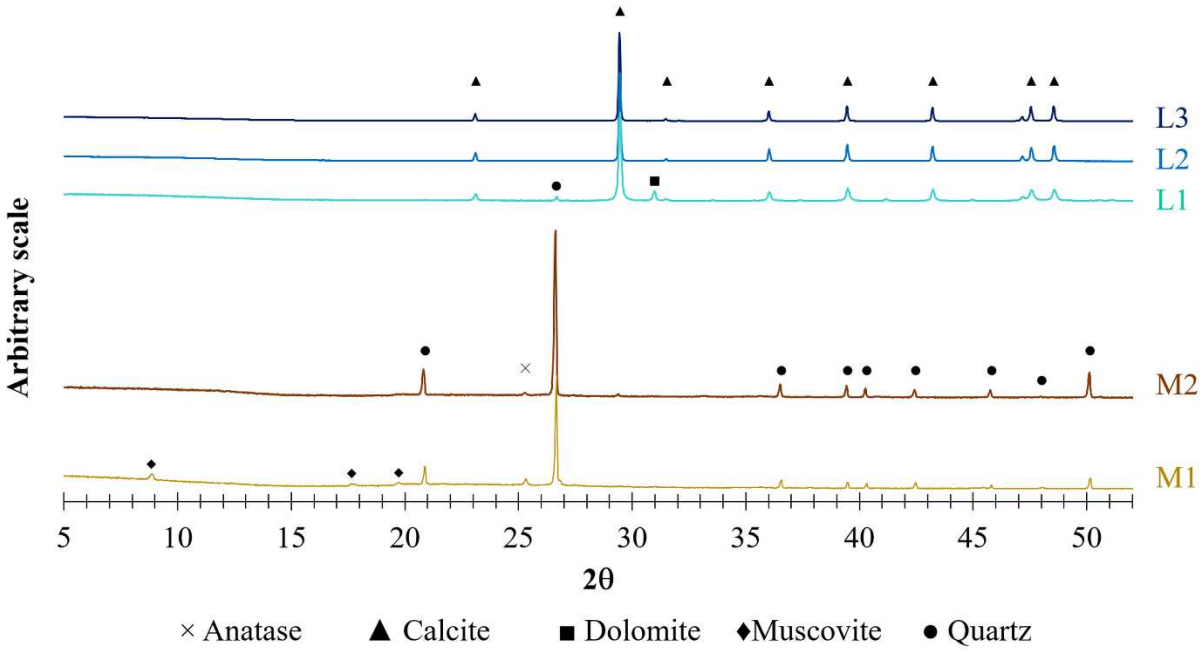

Figure 1: X-ray diffraction patterns of metakaolins and limestone fillers.

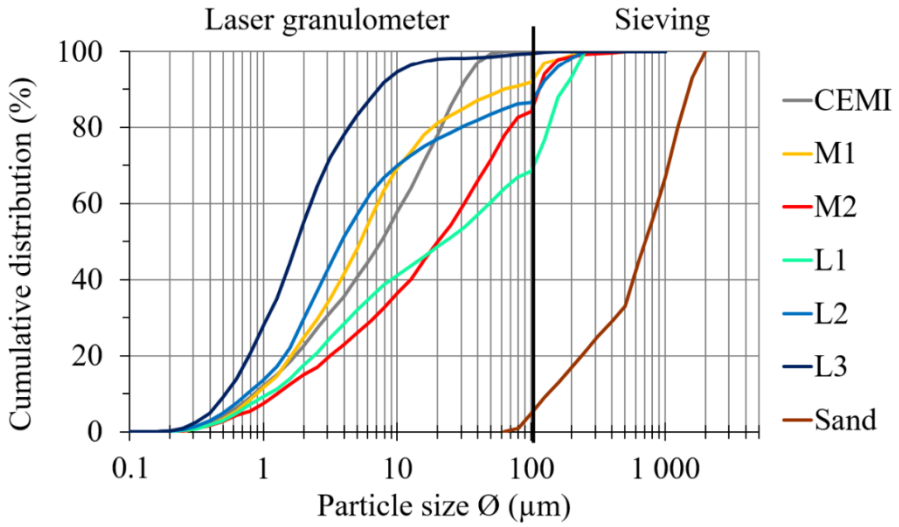

Figure 2: Experimental particle size distribution of both the powders and the sand (from the product technical file)

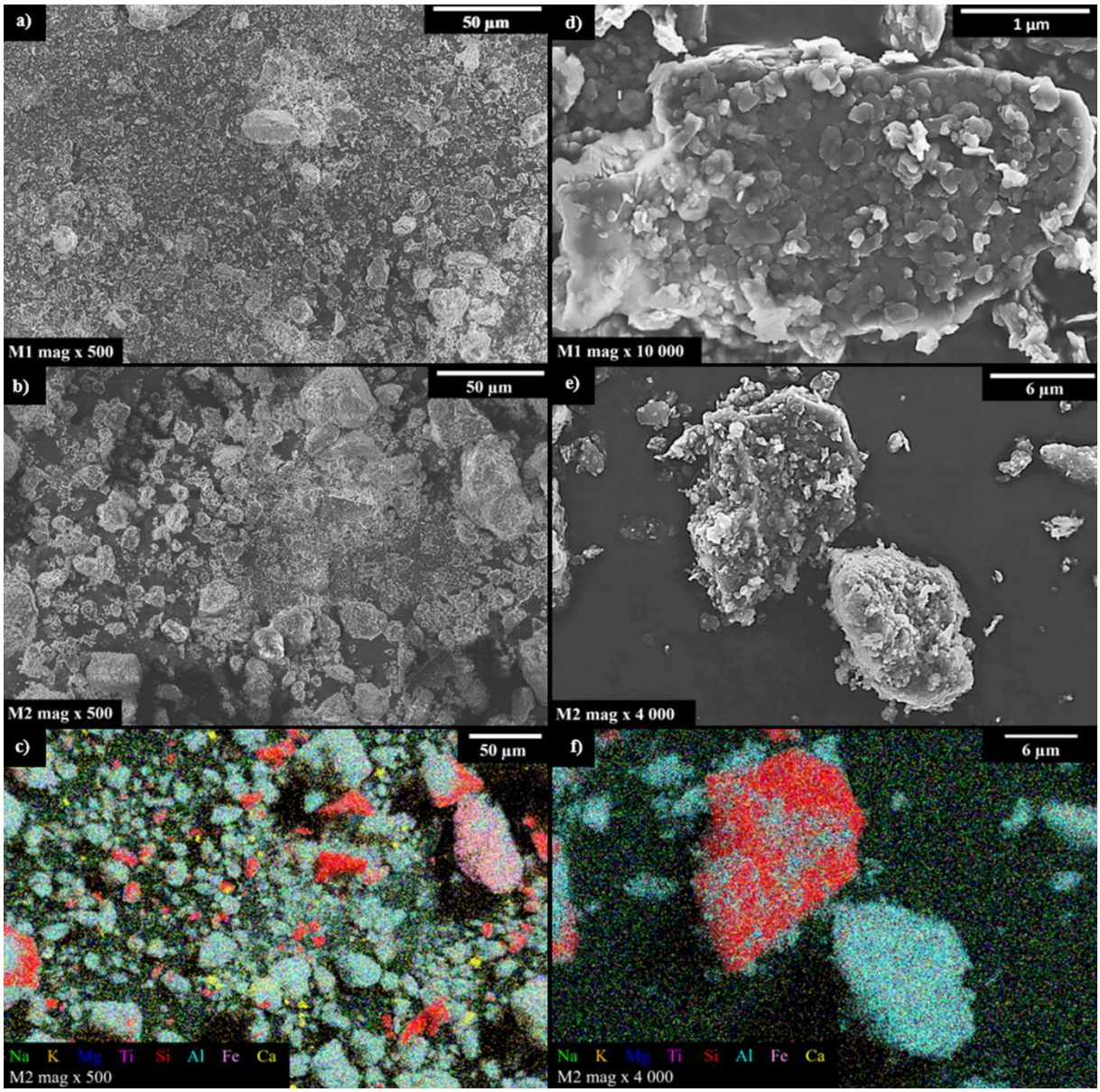

Figure 3: Observation with Scanning Electron Microscopy of metakaolin particles: a) Metakaolin M1 (mag ×500), b) metakaolin M2 (mag ×500), c) chemical analysis (EDS) of Fig. 3b, d) metakaolin M1 (mag ×10,000), e) metakaolin M2 (mag ×4,000) and f) chemical analysis of Fig. 3e

2.2 Experimental protocol

The experimental protocol followed to optimize the CEM I/MK/L binder packing density can be divided into three steps. The first is to determine the SCM packing density Φ on pastes of normal consistency. Knowing the packing density and particle size distribution y_i, the virtual packing density β_i of each SCM is calculated. This step has been detailed in the following section (2.2.1). During the second step, the evolution of the packing density of binary and ternary blends of the same consistency are simulated with the CPM and several points are verified experimentally (Section 2.2.2). The final step is dedicated to studying the properties of mortars with limestone and metakaolin. The packing

density of these mortars has been calculated for each composition with the CPM. The relationship between the packing densities of mortar and their spread is also demonstrated. Lastly, the mechanical strength of the studied mix designs have been measured at 7 and 28 days in order to evaluate the impact of additions on mechanical performance.

2.2.1 Packing density of the cement and additions with paste of normal consistency

As mentioned in the introduction, the scientific approach adopted in this study has been inspired by the study presented in [20]. Pastes of pure CEM I, binary or ternary blends were manufactured according to the method described in Standard NF EN 196-3 [21], which sets forth the protocol to obtain a paste with normal consistency. Any small variation around the optimal amount of water yields either a firm paste (a few millimeters of penetration) or too fluid a paste (full penetration). Thus, it is simple to accurately frame the value of the amount of water leading to a paste with the normal consistency sought.

The water/powder ratio (w/p) of the paste with normal consistency allows for the calculation of the real packing density (Φ) of the mineral skeleton by means of Equation (1).

For a mix containing *n* constituents, the specific gravity of the powder ρ_p is the sum of densities ρ_i of the cement and additions multiplied by their respective volumetric fraction x_i in the blend:

$$\rho_p = \sum_{i=1}^{n} x_i \rho_i \text{ with } \sum_{i=1}^{n} x_i = 1 \quad (4)$$

As part of this research protocol, a 250-cm^3 volume of paste, i.e. sufficient to fill the conical mold of 176.7 cm^3 and ensure an effective mix, was produced for each mix. The density of each paste (ρ_{exp}) was then calculated by weighing the filled mold, perfectly shaved and cleaned ($w_{cement\ paste}$), in order to check the quality of the mold filling and estimate the quantity of entrapped air (a%).

$$a\% = 1 - \frac{\rho_{exp}}{\rho_{th}} = 1 - \frac{\frac{w_{cement\ paste}}{V_{mould}}}{\sum_{i=1}^{n} x_i \rho_i} \quad (5)$$

To define a mix design, it is necessary to assign the respective volume fractions x_c and x_a of the constituents as well as the amount of water required. The calculation of the weight of each constituent is shown step-by-step below:

- the real volume V_p of dry powder to pour into the mixer:

$$V_p = \frac{250-w}{1+(x_c\rho_c+x_a\rho_a)} \quad (6)$$

- the weight of cement c and of admixture a (in grams):

$$c = V_p x_c \rho_c \text{ and } a = V_p x_a \rho_a \quad (7)$$

- with the specific gravity of both the mineral additions ρ_a and cement ρ_c.

Due to the coarser granular distribution of the standardized sand, its packing density cannot be determined in the same way as that used for cements and mineral additions. The real packing density of the standardized sand was thus determined with the following equation:

$$\Phi_{Sand} = \frac{V_{th}}{V_{exp}} \text{ with } V_{th} = \frac{w_{sand}}{\rho_{sand}} \quad (8)$$

where w_{sand} and ρ_{sand} correspond respectively to the weight and density of the sand.

The real volume V_{exp} occupied by a bag of normalized sand, with a weight of 1,350 g, was experimentally measured. For this measurement, the complete bag was filled in a 2-liter cylindrical container subsequently vibrated for one minute with a stress applied on the top of the sand bed (10 kPa) to ensure compaction. The packing index associated with this process is: K=9.

2.2.2 Determination of the virtual packing density βi

The virtual packing density of the various mixes was calculated by applying the Compressible Packing Model (CPM) using Equations (2) and (3), with a packing index K equal to 4.8, as determined in [20] and confirmed in [22]. Let's recall that the input parameters necessary to calculate the virtual packing

density β_i are: the particle size distribution y_i, and the experimental packing density Φ of each pure constituent included in the mix.

For this study, the evolution in the packing density of binary blends (CEM I and one addition) was first modeled. This initial step sought to determine the influence of additions on packing density, i.e. whether they exhibit a positive or a negative impact on the packing density of a mix with CEM I. Next, the same approach was followed for ternary blends. Thus, the impact of two additions in a ternary blend can be characterized, while assessing which addition has the greater impact. Furthermore, experimental values are compared to the theoretical curves in order to verify the relevance of CPM in the case of limestone calcined clay binder.

2.2.3 Relationship with mortar in the fresh state

To correlate the value of packing density both experimentally and numerically obtained with rheology behavior in the fresh state, several mortars were manufactured. As for the pastes, the cement substitution proceeded in volume. The mortar formulation parameters are displayed in Table 2 when metakaolin M1 or M2 is used (identical density). The mixing protocol, plus the sand and water weights all conform to Standard NF EN 196-1 [33]. The amounts of cement and additions were calculated from a volume of powder set at 150 cm^3, corresponding to the volume of a cement with an average density of 3 g/cm^3 used to manufacture a standardized mortar [33]. The volume and weight of cement and additions was calculated with their respective density.

The spread of fresh mortars was measured with a shaking table according to the protocol described in Standard NF EN 1015-3 [34]. Moreover, the compressive strengths of the mortar specimens ($4 \times 4 \times 16$ cm^3) at both 7 and 28 days were measured.

Table 2: Mortar formulation parameters with metakaolin M1.

	M1-15% L1-30%	*M1-15% L2-30%*	*M1-15% L3-30%*	*M1-30% L1-30%*	*M1-30% L2-30%*	*M1-30% L3-30%*
$V_{CEM\ I}$ (cm^3) / $w_{CEM\ I}$ (g)	82.5 / 263.01			60 / 1 912.28		
V_{MK} (cm^3) / w_{M1} (g)	22.5 / 59.06			45 / 118.13		
V_L (cm^3)	45					
$w_L(g)$	123.75	121.5		123.75	121.5	
w_{sand} (g)	1 350					
w_{water} (g)	225					
w_{sand}/w_{binder}	3.03	3.04		3.12	3.13	
w_{water}/w_{binder}	0.5	0.51		0.52		

3. Results

3.1. Real and virtual packing densities of the raw materials

The w/b ratio of CEM I is equal to 0.298 according to Table 3. For the additions (metakaolin or limestone filler), it is not recommended to manufacture a paste without CEM I due to the pH and alkalinity imposed by the presence of cement. For this reason, two mixes were produced: the first with 80% vol. of additions and 20% vol. of CEM I, and the second with 90% vol. of additions and 10% vol. of CEM I. When metakaolins are used, the amount of water required to manufacture a paste with normal consistency considerably increases, while for limestone fillers the water demand is similar or decreases.

The real packing density (Φ) of these materials, as displayed in Table 3, was calculated using Equation 1. For the additions, the packing density value was determined for the two mixes at 80% vol. and 90% vol.; the packing density for 100% vol. could then be extrapolated by means of linear regression of the two previous points. The real packing density of metakaolins is low, Φ = 0.373 for metakaolin M1 and Φ = 0.456 for M2, thus revealing that these additions are decreasing the packing density. On the contrary, limestone fillers L1 and L2 are more compact than the CEM I, Φ = 0.652 and 0.571, respectively. However, the last limestone filler studied L3, the finest, did not exert the same influence on the mixture since the real packing density measured (Φ = 0.506) was lower than that of CEM I (Φ = 0.513), and the w/b ratio of the paste increased. Lastly, the normalized sand is a material with a very high real packing density (Φ = 0.781), as determined on vibrated dry packing.

According to the scientific approach laid out in this study, the next step consists of calculating by means of deconvolution the virtual packing density βi presented in Figure 4, via the implicit equation (2). The βi values are considered to be uniform over the entire granular spectrum of each material.

The βi of CEM I (0.427) lies within the range of values classically obtained without superplasticizer (0.41-0.44) [19].

Given the very low β_i and their PSD, the high amount of the two metakaolins studied should decrease the packing density when blended with CEMI. Metakaolin M1 has an unusually low virtual packing density for a granular material (β_i = 0.257). This value is similar to the β_i measured for silica fumes (β_i = 0.242) without superplasticizer [20]. This virtual packing density seems to be correlated with the morphology and texture of the grains, and therefore their specific surface area. The mineralogical nature, the surface charges of the grains and the water adsorption/absorption are also key parameters influencing the βi of powders. According to [19],

when the granular spectrum of a material is very thin (i.e. d50 less than several microns), the surface forces of the grains become predominant and oppose the natural tendency of spherical particles to stack properly. As a result, particles tend to form small loose clusters at the time of quenching, thus

leading to the formation of a mixture of low compactness. M1 is made up of a multitude of clay sheet agglomerates nested in one another (Figure 3d), which significantly increases the specific surface areas calculated with the BET method, i.e. 19.45 m²/g. The βi value of M2 equals 0.457; it is slightly higher by virtue of containing more coarse quartz particles covered with the clay sheets (Figures 3e, 3f); moreover, its specific surface area is slightly lower (15.95 m²/g).

The three limestone fillers all possess a βi value greater than that of CEM I, ranging from 0.47 to 0.51, as previously observed for limestone fillers [19].

The coarser the limestone particle size, the lower the specific surface area and the higher the virtual packing density. It is worth noting that L1 and M2 feature a similar particle size distribution (Figure 2) yet very different β_I values, thereby highlighting the importance of the particle's mineralogy and morphology.

The βi value of the normalized sand with a tight particle size distribution is the highest (0.704), lying close to that of a perfect arrangement of monosized spheres, as explained above (βi = 0.74). For a packing index K = 9, the real packing density of the monodisperse arrangement equals around 0.64, hence confirming the well-known values for randomly packed spheres.

In sum, βi offers a very interesting way to characterize the positive or negative effect of the addition on the packing density. With potential values ranging from 0.257 (M1) to 0.704 (sand), it allows distinguishing materials by taking into account several properties difficult to measure, e.g. morphology, and grain texture, surface charges and water adsorption.

Let's note that for the calculations, the powder water absorption was considered to be equal to 0. This is a key hypothesis since for porous materials, the water absorption would underestimate β_i, with water into the grain porosity being considered as intergranular porosity. However, it has been assumed in this study that the low value of β_i calculated for M1 or M2 essentially reflects its high water demand, its low packing density , and not its water absorption.

Table 3: Results of the experimental measurements of packing density of various binary blends (CEM I/addition) in order to extrapolate their packing density when pure.

	water/binder at normal consistency			*Real packing density Φ*		
Vol (%)	80%	90%	100%	80%	90%	100%
CEM I	-	-	0.298	-	-	0.513
M1	0.619	0.666	-	0.373	0.360	0.348
M2	0.396	0.424	-	0.481	0.469	0.456
L1	0.212	0.203	-	0.625	0.639	0.652
L2	0.274	0.274	-	0.567	0.571	0.575
L3	0.335	0.348	-	0.517	0.512	0.506
Sand	-	-	-	-	-	0.781

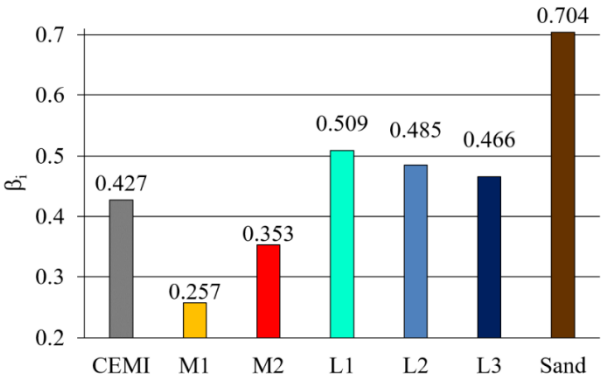

Figure 4: Virtual packing density β_i of each pure material studied.

3.2. Packing density of binary blends

Based on the virtual packing density (β_i) previously determined and the granular distribution (y_i) of the powder, the theoretical evolution of the packing density (Φ), at normal consistency (K=4.8), is displayed Figure 5 (continuous lines) as a function of the addition amount. The dots on this figure correspond to the experimental packing density. The error bars (± 0.01) correspond to the total deviation associated with the experimental packing density, with this value corresponding to a

variation of ± 2.5 g of water during the manufacturing of pastes, which is considered representative of test repeatability (mold filling, entrapped air, etc.). The origin of each curve is the same for each addition given that it is the packing density of the pure CEM I. The experimental and modeled packing densities are on the whole very close, thus underscoring the relevance of this methodology. Three trends can be observed:

- the first concerns the materials increasing the packing density, e.g. the two limestone fillers L1 and L2;
- the second trend relates to the intermediate behavior of L3, which displays a slight optimal packing density around 45% vol.;
- the final trend corresponds to materials decreasing the packing density, e.g. the two metakaolins M1 and M2.

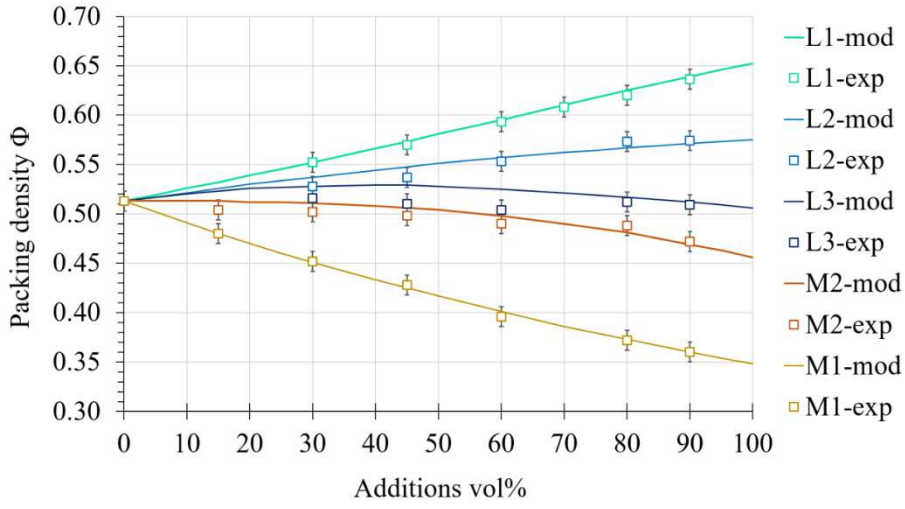

Figure 5: Evolution in the packing density of binary mixes with the amount of additions. The dots are the experimental values and the lines the numerical values modeled with the Compressible Packing Model (CPM)

According to Figure 5, the packing density of the CEM I/L1 mix increases almost linearly with the amount of L1. Indeed, the particle size distributions of CEM I and L1 are different and complementary (d50 = 7.5 µm vs. 60 µm, respectively), and the L1 grains have a better virtual packing density (β_i) than the cement grains. This result implies the nonexistence of an optimum and moreover that the packing density increases steadily as the amount of L1 in the mix increases from 0% to 100%.

Limestone filler L2 also improves the packing density since the Φ value of the CEM I/L2 mixture increases continuously with the amount of L2. However, this increase in packing density is less than with the L1 filler (CEM 1/L1) because the particle size distribution of the two materials (CEM I/L2) is rather similar (Figure 2), with a d50 of 7.5 µm and 3.8 µm, respectively. Also, the virtual packing density βi of their grains is less contrasted than previously (Figure 4). These two parameters do not favor as large an increase in packing density as in the previous case. They therefore explain why limestone filler L2 is less effective than L1 at increasing the packing density of these binary mixtures.

When the amount of L3 is less than 45% vol., the packing density of the CEM I/L3 blend slightly increases. Since the β_i values of L3 and CEM I are similar, the fineness of L3 (d50 = 1.8 µm) serves to explain this trend. Therefore, when the mix contains a small amount of L3, the packing density increases moderately due to the effect of the β_i of L3 grains. When the mixture contains a high proportion of L3, the packing density decreases due to the fine L3 fraction.

The evolution in packing density vs. the amount of metakaolins shows a different behavior. It can be seen in Figure 5 that M2 exerts an negative effect on the packing density of CEM I/M2 mixture when the amount exceeds 45% vol. because of the low β_i value (0.353). However, for low percentages, the PSD of M2 and CEM I are complementary (Figure 2) and reduce the negative impact of the M2 β_i. Metakaolin M1 has the highest negative effect on the packing density (β_i = 0.257); its PSD lies close to that of CEM I. These two criteria do not favor an increase in packing density when the two products are mixed.

In conclusion, in binary blends, limestone fillers improve the packing density whereas metakaolins decrease it. This result is explained by their respective β_i values, but interaction between the PSD of the two ingredients also has a significant influence on the packing density of the binary mix. The tendencies observed in this section are confirmed in the presence of superplasticizers by the preliminary results described in Appendix concerning the effect of superplasticizers on the paste packing density. The topic of the next section pertains to verifying these observations on ternary blends, wherein limestone fillers could offset the strong negative characteristic of metakaolins.

3.3. Packing density of ternary blends

Ternary diagrams showing the evolution in packing density vs. the composition have been drawn (Figure 6). In the simulation, the CEM I content varied between 100% and 40% vol., which provides a realistic floor value for a calcined clay limestone binder. Consequently, the content of metakaolin and/or limestone filler never exceeded 60% vol. Figures 6a, 6c and 6e display the ternary diagrams modeled when metakaolin M1 was used with L1, L2 and L3, respectively. Figures 6b, 6d and 6f correspond to the similar blends with M2. The large black dots on the diagrams indicate mixtures whose packing density has been measured experimentally and compared to the calculated values (Figures 5 and 7).

Those binders having the same packing density as pure CEM I ($\Phi \approx 0.513$) are indicated in a shaded white color on each diagram. The higher the packing density, the lower the water demand (w/(c+a)) of the mix and the greener the ternary diagrams. On the contrary, the redder the ternary diagrams, the lower the packing density and the higher the water demand of the blend.

The majority of mixes incorporating M1 (Figures 6a, 6c, 6e) have a lower packing density (yellow to red colors) than those incorporating M2 (Figures 6b, 6d, 6f, green). The nature of the limestone filler has less impact on packing density. Thus, for example:

- To maintain the same packing density (i.e. water demand) of the cement alone (white color, $\Phi = 0.513$), a ternary blend incorporating metakaolin M1 only need contain a maximum of:
    - 20% vol. metakaolin and at least 30% vol. L1 filler,
    - 15% vol. metakaolin and at least 30% vol. L2 filler,
    - 10% vol. metakaolin and at least 20% vol. L3 filler.

  Any combination incorporating more metakaolin M1 will lead to a lower packing density. It is straightforward to understand that these binders will perform poorly without superplasticizer.

- For ternary mixes incorporating metakaolin M2, the cement packing density is always achieved or even slightly exceeded, regardless of metakaolin content. The type of limestone filler only has a somewhat marginal influence. For example, a blend containing 30% vol. of M2 and 20% vol. of:
    - L3 will have a packing density of 0.52,
    - L2 will have a packing density of 0.53,
    - L1 will have a packing density of 0.55.

Thus, L1, the coarser limestone with the highest packing density, has the most favorable influence.

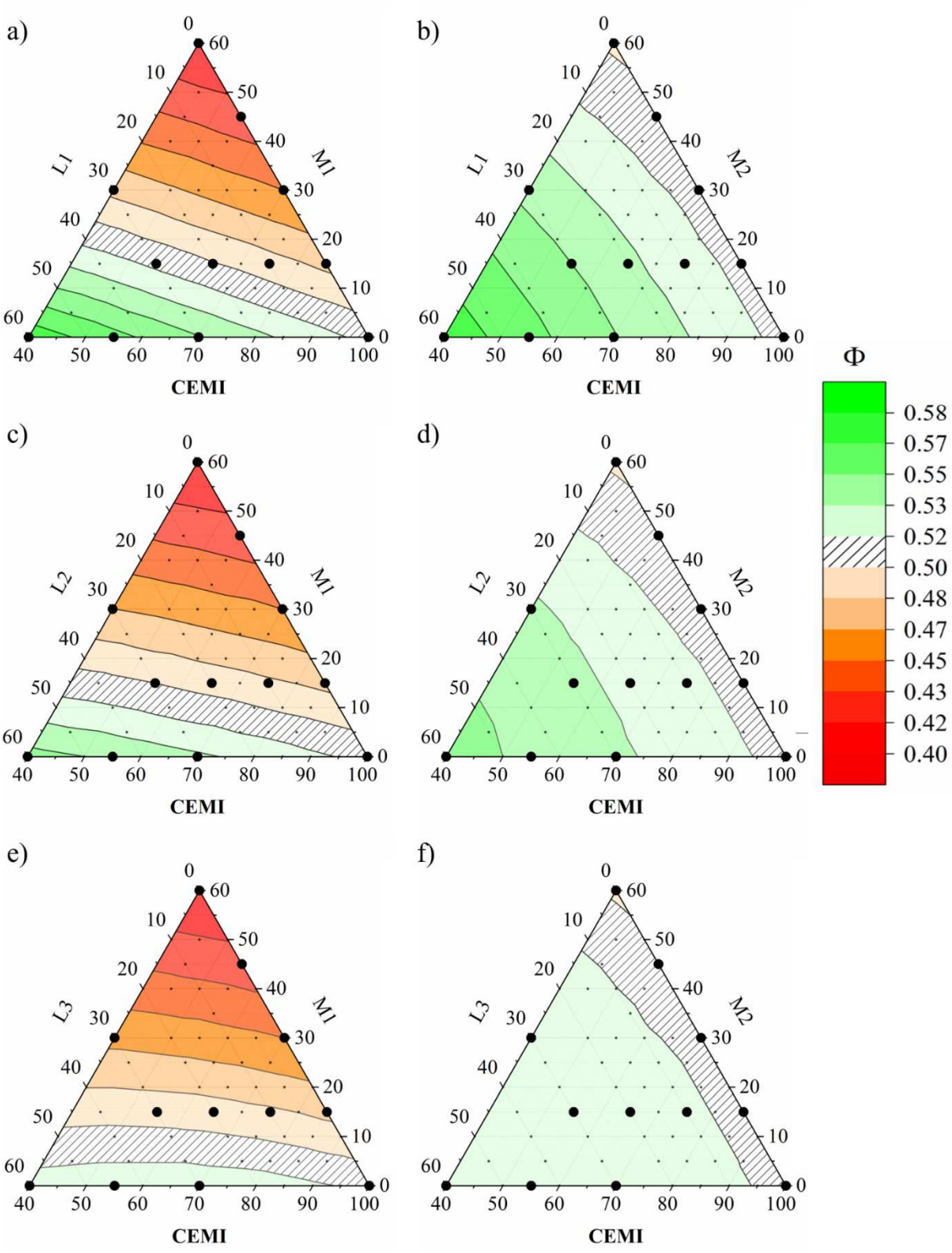

Figure 6: Evolution in packing density of ternary blends. The small dots correspond to the packing density of mixes calculated by the CPM while the larger dots indicate the experimentally measured packing density.

In sum, the strongest impact on packing density stems from the type of metakaolin used (M1 or M2). Limestone fillers always exert a positive influence, but their PSD only seems to have a moderate impact.

Figure 7 displays the evolution in packing density for ternary blends as a function of the amount of limestone fillers for a fixed amount of metakaolin, i.e. 15% vol. (Figure 7a) and 30% vol. (7b). The continuous lines correspond to the values calculated by the CPM, while the dots reflect the experimental data, for both M1 (in blue) and M2 (red).

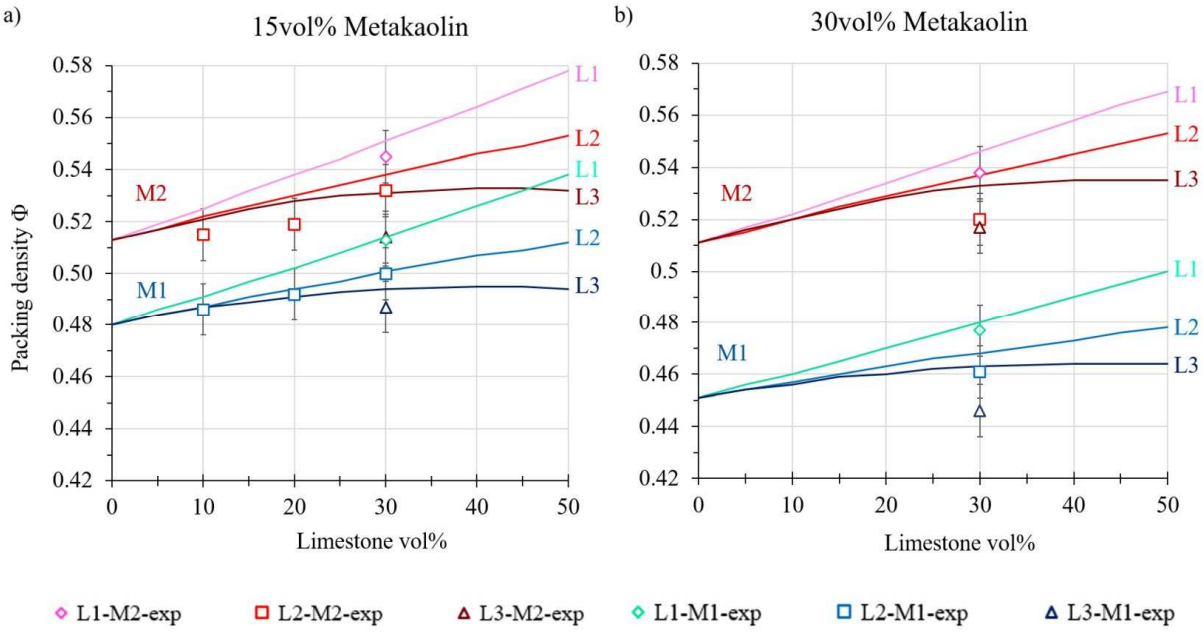

Figure 7: Evolution in packing density (Φ) vs. the amount of limestone in a ternary blend: a) with 15%vol of metakaolin and b) with 30%vol of metakaolin.

The modeled curves displayed in Figure 7a show that whether M1 or M2 is involved, the difference between the types of limestone used is only significant as of a substitution rate equal to 30% vol. This influence has been confirmed by experimental measurements.

The ratio w/(c+a) can be calculated from the value of the packing density, either modeled or measured, with the following equation:

$$\frac{w}{(c+a)} = \left[\left(\left(\frac{1}{\Phi}\right) - 1\right) \times \left(\left(\frac{x_a}{\rho_a}\right) + \left(\frac{x_b}{\rho_b}\right) + \left(\frac{x_c}{\rho_c}\right)\right)\right] \quad (9)$$

where x_a, x_b and x_c are the volumetric proportions of each blend constituent and ρ_a, ρ_b and ρ_c their density.

For example, with 30% vol. of metakaolin and limestone, between the blend containing M1 and M2, a difference of around 0.075 in the w/(c+a) ratio is obtained. When M1 is used, the influence of limestone type is limited since the water/binder ratio will only change by roughly 0.027 between L1 and L3.

The influence of the limestone and metakaolin in the mortar will now be discussed through an assessment of packing density, spread and mechanical strength.

3.4. Properties of mortars

3.4.1 Packing density

The packing density of mortars (Φ_M), containing 1,350 g of sand blended with a constant volume of various ternary CEM I/MK/L binders, has been calculated with the CPM (Figure 8). For mortars, the packing density (Φ_M) and packing index (K) are modeled based on mortar composition (Table 2), PSD (Figure 2) and the virtual packing density (β_i), as previously determined (Figure 4).

In comparison with the pastes at normal consistency (K = 4.8), as previously modeled (Section 3.3) with the same volume fraction of additions, the packing index of the mortars calculated with the model lies between 4.69 and 5.66, hence rather close to the packing index of the paste, i.e. equal to 4.8.

The packing density of the mortars ($0.79 < \Phi_M < 0.83$) is much higher than that of the pastes ($0.44 < \Phi < 0.55$) mainly due to the high proportion of sand (Table 2), which contains coarser particles with a very high virtual packing density (Figure 4). In the mixes chosen herein, the high proportion of sand also reduces the effect of the binder, which in turn explains why the variation in mortar packing density is limited to 0.04 instead of 0.11 for the paste made with the same binders. However, the influence of metakaolin type (M1 in blue or M2 in red) and its quantity (15% vol. vs. 30% vol.) remains clearly visible in the packing density of mortars (i.e. $\Phi_{M\text{-}M1\text{-}3030} < \Phi_{M\text{-}M1\text{-}1530} < \Phi_{M\text{-}M2\text{-}3030} \leq \Phi_{M\text{-}M2\text{-}1530}$). For mortars, the impact of limestone type on packing density is small (around 0.01), yet it is

interesting to observe that the higher Φ_M is reached systematically with the finest limestone (L3) instead of the coarser one (L1) for the packing density of pastes (Φ). Although the β_i value of L3 is low, its complementarity PSD with the sand improves the packing density of the mortar.

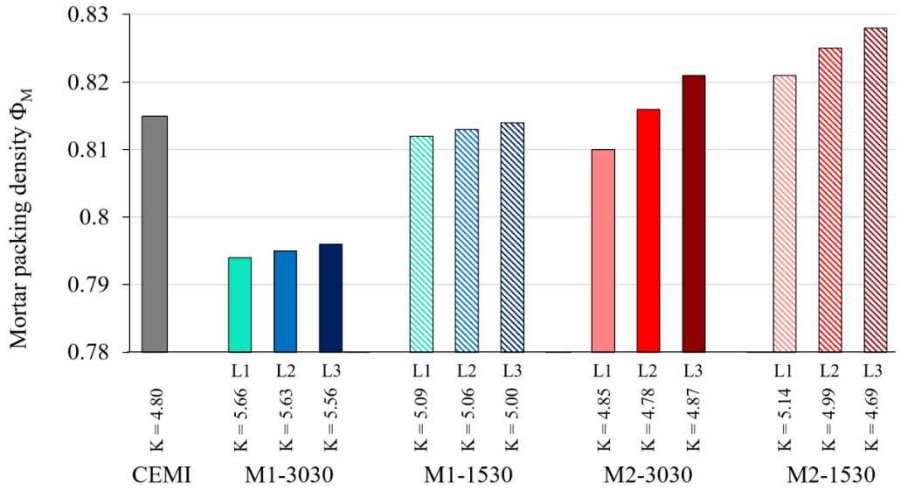

Figure 8: Evolution of the packing index of mortar vs. its composition.

3.4.2. Spread

The correlation between the calculated mortar packing density and the measured spread is shown in Figure 9. For the same amount of MK (15% or 30%), the spread of mortars with a low packing density (i.e. containing M1, in blue) is 2-4 cm below that with the highest packing density (i.e. containing M2, in red). Let's note that the type of limestone used only impacts the spread very slightly (± 10 mm), most likely due to its limited effect on the mortar packing density (around 0.01). These tests on mortars demonstrate that despite the low virtual packing density of metakaolins, blends with a spread greater than or equal to CEM I can be manufactured, especially when 30% vol. of limestone is added.

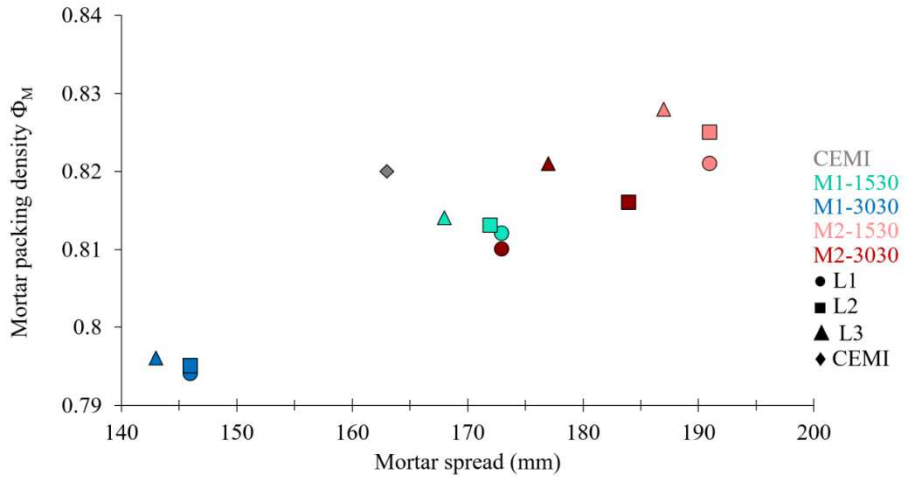

Figure 9: Comparison between the wet packing density of mortar modeled (Φ_M) and its experimentally measured spread.

3.4.3. Compressive strength

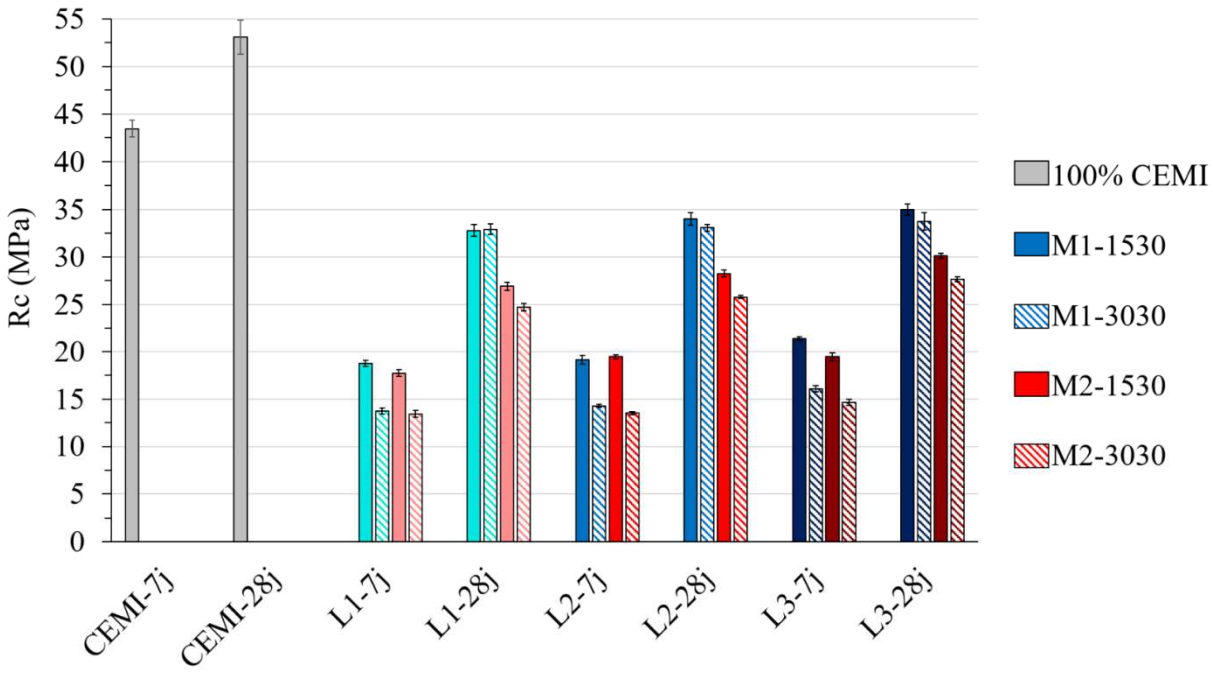

Figure 10: Results of the compressive strength of mortars at 7 and 28 days.

The compressive strength of mortars (Figure 10) was measured at both 7 and 28 days. The compressive strength with additions is significantly less (≈ 20 MPa) than the compressive strength of the reference with 100% CEM I. This finding mainly stems from the high limestone proportion (30% vol.), as well as the slightly higher water/binder ratio with additions due to the cement volume substitution (Table 2).

The metakaolin used has a major impact on compressive strength, whether 45% vol. or 60% vol. of the CEM I is substituted, as the M1 compressive strength is 5-8 MPa higher than blends with M2. For M1, given the low CEM I proportion in the blend, the strength reached at 28 days (> 32.5 MPa) underscores the high purity and reactivity of this metakaolin, hence the industrial interest in these binders.

The type of limestone has a smaller impact on mortar strength (≈ 2 MPa), but for each milestone (7 and 28 days), maximum strength is reached when the finest limestone is used (L3) and thus when Φ_M is highest. Moreover, the greater specific surface area of the limestone could increase the kinetics and amount of monocarboaluminate hydrates formed during the reaction [35].

4. Conclusion

This article has investigated the packing density of CEM I/MK/L ternary binders. The CPM and tests conducted on pastes with two metakaolins and three different types of limestone have shown that limestone fillers display a higher virtual packing density β_i (0.509) than CEM I (0.427), whereas the virtual packing density of metakaolins is really low β_i (reaching 0.257). The virtual packing density parameter allows considering the physical and chemical specificities of metakaolins and moreover characterizes their negative impact on the packing density. Using the CPM, the packing density (Φ) of binary or ternary blends can be predicted. When binary or ternary blends are manufactured, the type of metakaolin used exerts a great influence on both the packing density and cement paste water demand. Added limestone always has a positive influence on packing density because it compensates for the low β_i value of metakaolin. On CEM I/MK/L pastes, the coarser filler (L1) has the highest packing density, but the PSD of the selected limestone only seems to have a moderate influence. The impact from the type of metakaolin employed is also clearly visible in the packing density of mortars and their spread. In mortars, the compressive strength and packing density are slightly higher with the finest limestone (L3), yet its effect on spread remains insignificant.

Using these results, it has been possible to prepare ternary CEM I/MK/L binders for mortars featuring an adjusted spread and a compressive strength close to 32.5 MPa at 28 days when up to 60% vol. of CEM I is substituted. Experiments teased in Appendix are ongoing to determine the effect of superplasticizers on the metakaolin packing density. These results will contribute to optimize the mix design of concretes containing this kind of environmentally friendly ternary binders.

Acknowledgments

This study has been supported by the CO2REDRES project, which is funded by the European Union's INTERREG Grande Région program (IP 4-08-185). The authors are grateful to Sébastien Fontana from Jean Lamour Institute for realizing the measurements of specific surface area of the materials by BET method.

References

[1] M. Murat and C. Comel, 'Hydration reaction and hardening of calcined clays and related minerals III. Influence of calcination process of kaolinite on mechanical strengths of hardened metakaolinite', *Cement and Concrete Research*, vol. 13, no. 5, pp. 631–637, Sep. 1983, doi: 10.1016/0008-8846(83)90052-2.

[2] C. He, B. Osbaeck, and E. Makovicky, 'Pozzolanic reactions of six principal clay minerals: Activation, reactivity assessments and technological effects', *Cement and Concrete Research*, vol. 25, no. 8, pp. 1691–1702, Dec. 1995, doi: 10.1016/0008-8846(95)00165-4.

[3] B. B. Sabir, S. Wild, and J. Bai, 'Metakaolin and calcined clays as pozzolans for concrete: a review', *Cement and Concrete Composites*, vol. 23, no. 6, pp. 441–454, Dec. 2001, doi: 10.1016/S0958-9465(00)00092-5.

[4] P. S. L. Souza and D. C. C. Dal Molin, 'Viability of using calcined clays, from industrial by-products, as pozzolans of high reactivity', *Cement and Concrete Research*, vol. 35, no. 10, pp. 1993–1998, Oct. 2005, doi: 10.1016/j.cemconres.2005.04.012.

[5] C. A. Love, I. G. Richardson, and A. R. Brough, 'Composition and structure of C–S–H in white Portland cement–20% metakaolin pastes hydrated at 25 °C', *Cement and Concrete Research*, vol. 37, no. 2, pp. 109–117, Feb. 2007, doi: 10.1016/j.cemconres.2006.11.012.

[6] T. Matschei, B. Lothenbach, and F. P. Glasser, 'The role of calcium carbonate in cement hydration', *Cement and Concrete Research*, vol. 37, no. 4, pp. 551–558, Apr. 2007, doi: 10.1016/j.cemconres.2006.10.013.

[7] B. Lothenbach, G. Le Saout, E. Gallucci, and K. Scrivener, 'Influence of limestone on the hydration of Portland cements', *Cement and Concrete Research*, vol. 38, no. 6, pp. 848–860, Jun. 2008, doi: 10.1016/j.cemconres.2008.01.002.

[8] R. Fernandez, F. Martirena, and K. L. Scrivener, 'The origin of the pozzolanic activity of calcined clay minerals: A comparison between kaolinite, illite and montmorillonite', *Cement and Concrete Research*, vol. 41, no. 1, pp. 113–122, Jan. 2011, doi: 10.1016/j.cemconres.2010.09.013.

[9] M. Antoni, J. Rossen, F. Martirena, and K. Scrivener, 'Cement substitution by a combination of metakaolin and limestone', *Cement and Concrete Research*, vol. 42, no. 12, pp. 1579–1589, Dec. 2012, doi: 10.1016/j.cemconres.2012.09.006.

[10] G. Cardinaud, E. Rozière, O. Martinage, A. Loukili, L. Barnes-Davin, M. Paris and D. Deneele, 'Calcined clay – Limestone cements: Hydration processes with high and low-grade kaolinite clays', *Construction and Building Materials*, vol. 277, p. 122271, Mar. 2021, doi: 10.1016/j.conbuildmat.2021.122271.

[11] K. Scrivener, F. Avet, H. Maraghechi, F. Zunino, J. Ston, W. Hanpongpun and A. Favier, 'Impacting factors and properties of limestone calcined clay cements (LC^3)', *Green Materials*, vol. 7, no. 1, pp. 3–14, Mar. 2019, doi: 10.1680/jgrma.18.00029.

[12] F. Avet, E. Boehm-Courjault, and K. Scrivener, 'Investigation of C-A-S-H composition, morphology and density in Limestone Calcined Clay Cement (LC3)', *Cement and Concrete Research*, vol. 115, pp. 70–79, Jan. 2019, doi: 10.1016/j.cemconres.2018.10.011.

[13] K. Scrivener, F. Martirena, S. Bishnoi, and S. Maity, 'Calcined clay limestone cements (LC3)', *Cement and Concrete Research*, vol. 114, pp. 49–56, Dec. 2018, doi: 10.1016/j.cemconres.2017.08.017.

[14] AFNOR, 'Cement - Part 5 : portland-composite cement CEM II/C-M and Composite cement CEM VI (NF EN 197-5)', May 2021.

[15] AFNOR, 'Concrete - Specification, performance, production and conformity - National addition to the standard NF EN 206 (NF EN 206/CN)', Dec. 2014.

[16] P. Hawkins, P. D. Tennis, and R. J. Detwiler, 'The Use of Limestone in Portland Cement: A State of the Art Review', Portland Cement Association, Skokie, Illinois, USA, EB227, 2005.

[17] L. Courard, D. Herfort, and Y. Villagrán, 'Limestone Powder', in *Properties of Fresh and Hardened Concrete Containing Supplementary Cementitious Materials*, vol. 25, N. De Belie, M. Soutsos, and E. Gruyaert, Eds. Cham: Springer International Publishing, 2018, pp. 123–151. doi: 10.1007/978-3-319-70606-1_4.

[18] S. Wild, J. M. Khatib, and A. Jones, 'Relative strength, pozzolanic activity and cement hydration in superplasticised metakaolin concrete', *Cement and Concrete Research*, vol. 26, no. 10, pp. 1537–1544, Oct. 1996, doi: 10.1016/0008-8846(96)00148-2.

[19] F. de Larrard, *Concrete mixture proportioning a scientific approach, modern concrete technology*. In: Mindess S, Bentur A, editors, vol. 9. E&FN Spon, London; 1999

[20] A. Lecomte, J.-M. Mechling, and C. Diliberto, 'Compaction index of cement paste of normal consistency', *Construction and Building Materials*, vol. 23, no. 10, pp. 3279–3286, Oct. 2009, doi: 10.1016/j.conbuildmat.2009.05.005.

[21] AFNOR, 'Methods of testing cement - Part 3 : determination of setting time and soundness (NF EN 196-3)', 2017.

[22] T. Sedran, F. de Larrard, and L. Le Guen, 'Détermination de la compacité des ciments et additions minérales à la sonde de Vicat', *Bulletin des Laboratoires des Ponts et Chaussées*, no. 270–271, pp. 155–163, 2007.

[23] H. H. C. Wong and A. K. H. Kwan, ‘Packing density of cementitious materials: part 1—measurement using a wet packing method’, *Mater Struct*, vol. 41, no. 4, pp. 689–701, May 2008, doi: 10.1617/s11527-007-9274-5.

[24] A. K. H. Kwan and W. W. S. Fung, ‘Packing density measurement and modelling of fine aggregate and mortar’, *Cement and Concrete Composites*, vol. 31, no. 6, pp. 349–357, Jul. 2009, doi: 10.1016/j.cemconcomp.2009.03.006.

[25] G. Marchetti, E. F. Irassar, and V. F. Rahhal, ‘Effects of packing density and water film thickness on fresh and hardened properties of ternary cement pastes’, *Advances in Cement Research*, vol. 32, no. 10, pp. 444–455, Oct. 2020, doi: 10.1680/jadcr.18.00133.

[26] G. Marchetti, V. F. Rahhal, and E. F. Irassar, ‘Influence of packing density and water film thickness on early-age properties of cement pastes with limestone filler and metakaolin’, *Mater Struct*, vol. 50, no. 2, p. 111, Apr. 2017, doi: 10.1617/s11527-016-0979-1.

[27] A. B. Yu, J. Bridgwater, and A. Burbidge, ‘On the modelling of the packing of fine particles’, *Powder Technology*, vol. 92, no. 3, pp. 185–194, Aug. 1997, doi: 10.1016/S0032-5910(97)03219-1.

[28] A. K. H. Kwan, K. W. Chan, and V. Wong, ‘A 3-parameter particle packing model incorporating the wedging effect’, *Powder Technology*, vol. 237, pp. 172–179, Mar. 2013, doi: 10.1016/j.powtec.2013.01.043.

[29] A. K. H. Kwan, V. Wong, and W. W. S. Fung, ‘A 3-parameter packing density model for angular rock aggregate particles’, *Powder Technology*, vol. 274, pp. 154–162, Apr. 2015, doi: 10.1016/j.powtec.2014.12.054.

[30] K. W. Chan and A. K. H. Kwan, ‘Evaluation of particle packing models by comparing with published test results’, *Particuology*, vol. 16, pp. 108–115, Oct. 2014, doi: 10.1016/j.partic.2013.11.008.

[31] W. Du, M. Li, Z. Pei, and C. Ma, ‘Performances of three models in predicting packing densities and optimal mixing fractions of mixtures of micropowders with different sizes’, *Powder Technology*, vol. 397, p. 117095, Jan. 2022, doi: 10.1016/j.powtec.2021.117095.

[32] AFNOR, ‘Methods of testing cement - Determination of fineness (NF EN 196-6)’, Dec. 2018.

[33] AFNOR, ‘Methods of testing cement - Part 1: determination of strength (NF EN 196-1)’, Sep. 2016.

[34] AFNOR, ‘Methods of test for mortar for masonry - Part 3 : determination od consistence of fresh mortar (by flow table) (NF EN 1015-3)’, Oct. 1999.

[35] G. D. Moon, S. Oh, S. H. Jung, and Y. C. Choi, ‘Effects of the fineness of limestone powder and cement on the hydration and strength development of PLC concrete’, *Construction and Building Materials*, vol. 135, pp. 129–136, Mar. 2017, doi: 10.1016/j.conbuildmat.2016.12.189.

Appendix: Superplasticizer demand of cement and additions

This part of the study is performed by measuring the increase of packing density Φ when various proportions of superplasticizer (SP) are added in the cement paste. The SP* saturation dosage is the one for which the packing density does not increase anymore despite the addition of superplasticizer.

Protocol

Considering the rheological effect of the superplasticizer, the protocol allowing to obtain mixtures with same consistency had to be adapted. Indeed, this admixture confers a quasi-viscous behaviour to the suspension (disappearance of the shear threshold) which makes illusory a stabilization of the probe at 6mm from the bottom of the mold (normal consistency). Moreover, its presence requires a greater mixing energy for the "coalescence" to take place. The water demand used to calculate Φ (Equation 1) is then the one allowing to obtain a smooth viscous paste after the conventional application of 3 mixing cycles. A slightly lower amount of water leaves the mixture in a wet soil state; a slightly higher amount of water results in a very fluid paste before the completion of mixing. The water provided by the superplasticizer is taken into account in the water demand.

In a first step, the saturation dosage SP* of the cement alone is sought. It is defined empirically as the quantity of superplasticizer that provides 95% of the increase of the packing density (difference between the packing density without SP and the maximum packing density reached with SP). The packing density at SP* is noted Φ*.

In a second step, the saturation dosage of an addition is determined on mixes made with a small amount of cement to ensure high pH (90% addition and 10% cement, noted 90ADD-10C). For the different dosages of superplasticizer (SP/ADD), a SP quantity is also systemically added at the saturation dosage of the cement determined previously. The saturation dosage SP* of the addition is then determined as before (95% of the increase of the packing density), as well as the associated packing density Φ'.

Finally, the packing density Φ* of the addition alone is then calculated by linear interpolation of the packing density Φ' of the 90-10 mix and the packing density Φ' of a 80-20 mix made at saturation.

Results

The superplasticizer used in these tests is Chryso®Fluid Premia 525. Figure A.1 and Table A.1 show the results obtained:

- For cement alone, as expected, the effect of the superplasticizer at saturation (SP*/C=2.6%) results in a significant increase in the packing density (+23%);
- At saturation, M1 metakaolin requires a very large amount of superplasticizer (SP*/M1=6.4%). Its packing density highly increases (+43%) (considering its initial low packing density) but reaches barely the cement packing density without superplasticizer;
- Metakaolin M2 packing density increases moderately (+19%) with an intermediate saturation dosage (SP*/M2=3.5%);
- Saturation dosage of L2 limestone filler is very low (SP*/L2=1.2%) and induces a significant increase in its packing density (+29%).

Although made with only one superplasticizer, these tests show that the mineralogical nature and the fineness of the additions play a determining role in the saturation dosage and the SP impact on the packing density. They also confirm the other conclusions of the study, in the sense that the increases in packing density caused by the presence of the SP do not fundamentally change the behavior observed without superplasticizer (negative effect on the packing density of the metakaolin, etc.).

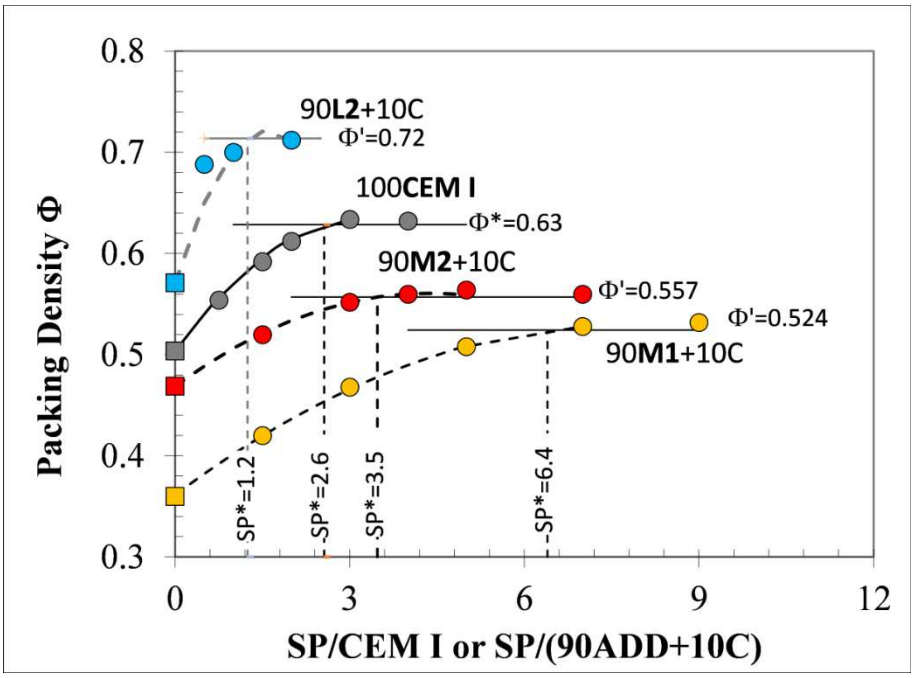

Figure A.1: Evolution in packing density of the cement and additions of the study vs. the dosage of superplasticizer. Saturation dosage SP and maximum compactness Φ* or Φ'*

Table A.1: Numerical results of the effect of the superplasticizer

	CEM	*M1*	*M2*	*L2*
Φ	0.513	0.348	0.456	0.575
SP/C or SP*/ADD (%)*	2.6	6.4	3.5	1.2
Φ*	0.63	0.497	0.542	0.743
(Φ–Φ)/Φ (%)*	23	43	19	29

Packing density of limestone clacined clay binder

Materials characterization

Materials		BET_{SSA} (m^2/g)	Virtual packing density (β_i)
Cement	CEM I	2.56	0.427
Limestones	L1	1.66	0.509
	L2	1.17	0.485
	L3	2.43	0.466
Calcined clays	M1	19.45	0.257
	M2	15.95	0.353

Compressible Packing Model (CPM)

$$K = \sum_{i=1}^{n} \frac{\frac{y_i}{\beta_i}}{\frac{1}{\Phi} - \frac{1}{\gamma_i}}$$

K = 4.8

y_i : volume fraction

γ_i : mixture virtual packing density

Modelling

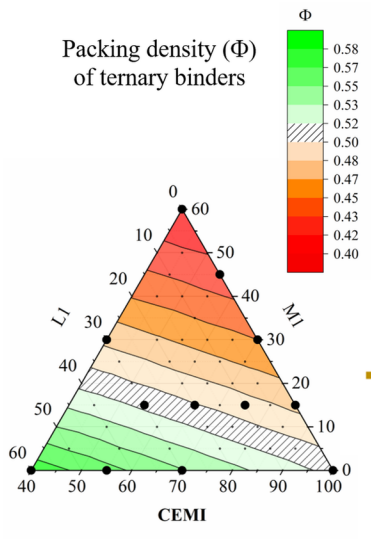

Experimental validation

Paste with normal consistency

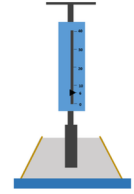

Mortar Spread